Rochelle salt piezoelectric coefficients obtained by x-ray multiple diffraction

2001 J. Phys.: Condens. Matter 13 10497

(http://iopscience.iop.org/0953-8984/13/46/318)

INSTITUTE OF PHYSICS PUBLISHING JOURNAL OF PHYSICS: CONDENSED MATTER

J. Phys.: Condens. Matter **13** (2001) 10497–10505 PII: S0953-8984(01)26132-3

Rochelle salt piezoelectric coefficients obtained by x-ray multiple diffraction

A O dos Santos[1], W H Yaegashi[1], R Marcon[1], B B Li[1], R V Gelamo[1], L P Cardoso[1], J M Sasaki[2], M A R Miranda[2] and F E A Mello[2]

[1] IFGW, UNICAMP, CP 6165, 13083-970 Campinas, SP, Brazil
[2] Dept Física, UFC, Campus do Pici, CP 6030, 60455-760 Fortaleza, Ceará, Brazil

Received 25 June 2001, in final form 27 September 2001
Published 2 November 2001
Online at stacks.iop.org/JPhysCM/13/10497

Abstract

In this paper, the theory of the method which uses the sensitivity and versatility of the multiple diffraction phenomenon to probe small lattice deformation induced by electric field (Avanci *et al* 1998 *Phys. Rev. Lett.* **81** 5426) was implemented to provide a relationship between the E-induced strain in the Rochelle salt (ferroelectric phase) crystal and the shift in the Renninger scan peak position. From that, all piezoelectric coefficients in a piezoelectric tensor row ($d_{21} = 7.0(6) \times 10^{-10}\,\mathrm{CN}^{-1}$, $d_{22} = 2.2(9) \times 10^{-9}\,\mathrm{CN}^{-1}$, $d_{23} = 2.1(9) \times 10^{-9}\,\mathrm{CN}^{-1}$ and $d_{25} = 3.7(8) \times 10^{-11}\,\mathrm{CN}^{-1}$) were determined by using the primary reflections (6 0 0) and (8 0 0) found as the best choices for the experiments with E parallel to the [0 1 0] direction (the b-axis).

1. Introduction

Rochelle salt, $NaKC_4H_4O_6 \cdot 4H_2O$, presents a ferroelectric phase between 255 and 297 K and a paraelectric phase out of this temperature range. The Rochelle salt structure [1] under the ferroelectric phase is monoclinic (space group $P2_111$, $a = 11.869(3)$ Å, $b = 14.316(8)$ Å, $c = 6.223(3)$ Å and $\beta = 89.26(4)^\circ$) and under the paraelectric phase it is orthorhombic (space group $P2_12_12$, $a = 11.880(3)$ Å, $b = 14.298(3)$ Å and $c = 6.216(2)$ Å).

Despite small resistance and low disintegration temperature, the Rochelle salt crystal has several important applications [2, 3], mainly in the acoustic field for its huge piezoelectric effect that is unapproached by any other known substance. The main scientific interest lies in its electric anomalies that are observed when an electric field is applied on the sample that causes slight structural deformations to it; this is called the converse piezoelectric effect.

The first quantitative measurements of the piezoelectric effect in Rochelle salt were made in 1894 by Pockels and his results are still in good agreement with those of later observers. The electrical anomalies of the Rochelle salt are confined to effects observed with the fields in the X-direction and shearing stresses in the YZ-plane. The piezoelectric constants d_{25} and

d_{36}, though larger than for most other crystals, do not exhibit special peculiarities, nor do the dielectric constants for the Y- and Z-directions [2].

The great difference in the piezoelectric coefficients for Rochelle salt has already been discussed in the literature and the most complex coefficient d_{14} is a typical parameter whose value can change one order of magnitude with varying temperature; this was investigated in detail in [4].

A method using the x-ray multiple diffraction (XRMD) phenomenon to assess small changes in the lattice parameters of meta-nitroaniline (mNA) nonlinear optical material under the application of electric field has already been presented in [5]. The method has become very useful and it has allowed for the determination of several mNA piezoelectric coefficients. Recently [6], it has also been applied successfully to the investigation of the MBNAP [(−)-2-(α-methylbenzylamino)-5-nitropyridine] nonlinear optical material. The importance of the method lies in its versatility in providing all coefficients in any piezoelectric tensor row just by performing one multiple diffraction pattern (Renninger scan).

In this paper, the XRMD method is applied to analyse the Rochelle salt and to obtain all the piezoelectric coefficients related to the application of the electric field parallel to the b-axis of this material. Here the necessary modifications in the calculations are also discussed to relate the electric field strength E, the strain ε_{ij}, the changes in the lattice parameters (Δa, Δb, Δc, $\Delta\beta$) and the changes of the peak positions in the x-ray patterns ($\Delta\omega^{00\ell}$, $\Delta\phi^{hk\ell}$) from which the piezoelectric coefficients are determined.

2. Theory

The application of a static, or quasi-static electrical field to a piezoelectric crystal generates strains in this crystal, which are the well-known converse piezoelectric effect [7]. The elements of the strain tensor ε_{ij} are linearly related to the applied electric field by

$$\varepsilon_{ij} = d_{ijk}E_k. \tag{1}$$

The analysis of the Rochelle salt, a monoclinic crystal which belongs to point group 2, can be started by writing the vectors representing the crystallographic axes in a orthogonal frame as

$$\vec{a} = (a_x, a_y, a_z) = (a\ \sin\beta,\ 0,\ a\ \cos\beta) \qquad \vec{b} = (0,\ b,\ 0) \qquad \vec{c} = (0,\ 0,\ c). \tag{2}$$

The changes in the length of any vector in this frame can be expressed in terms of the strain tensor, ε_{ij}, by differentiating the equations for the squared length of a vector and the cosine of the angle [6],

$$\Delta r = \frac{r_i r_j}{r}\,\varepsilon_{ij} \qquad \Delta\theta = \frac{1}{\sin\theta}\left[-\frac{r_i s_j + s_i r_j}{rs} + \cos\theta\left\{\frac{r^2 s_i s_j + s^2 r_i r_j}{(rs)^2}\right\}\right]\varepsilon_{ij}. \tag{3}$$

When Δr is applied in a separate form to each of the vector components one obtains

$$\Delta a = \frac{a_x a_x}{a}\varepsilon_{xx} + \frac{a_y a_y}{a}\varepsilon_{yy} + \frac{a_z a_z}{a}\varepsilon_{zz} + 2\frac{a_x a_y}{a}\varepsilon_{xy} + 2\frac{a_x a_z}{a}\varepsilon_{xz} + 2\frac{a_y a_z}{a}\varepsilon_{yz}. \tag{4}$$

By writing equation (1) in the matrix (Voigt) notation one obtains

$$\begin{pmatrix} \varepsilon_{xx} \\ \varepsilon_{yy} \\ \varepsilon_{zz} \\ 2\varepsilon_{yz} \\ 2\varepsilon_{zx} \\ 2\varepsilon_{xy} \end{pmatrix} = \begin{pmatrix} 0 & d_{21} & 0 \\ 0 & d_{22} & 0 \\ 0 & d_{23} & 0 \\ d_{14} & 0 & d_{34} \\ 0 & d_{25} & 0 \\ d_{16} & 0 & d_{36} \end{pmatrix} \begin{pmatrix} E_x \\ E_y \\ E_z \end{pmatrix}. \tag{5}$$

The lattice deformations of the case of $\vec{E} = E_y\hat{y}$ are given by

$$\varepsilon_{xx} = d_{21}E \qquad \varepsilon_{yy} = d_{22}E \qquad \varepsilon_{zz} = d_{23}E \qquad \varepsilon_{zx} = \left(\tfrac{1}{2}\right)d_{25}E. \tag{6}$$

Substituting the relationships obtained in (2) and (6) into equation (4) yields

$$\frac{1}{E_y}\frac{\Delta a}{a} = d_{21}\ \sin^2\beta + d_{23}\ \cos^2\beta + d_{25}\ \sin(2\beta). \tag{7}$$

Similarly, the changes in the other lattice parameters are expressed by

$$\frac{1}{E_y}\frac{\Delta b}{b} = d_{22} \tag{8}$$

$$\frac{1}{E_y}\frac{\Delta c}{c} = d_{23}. \tag{9}$$

The change in the β angle is obtained from the application of equation (2):

$$\frac{1}{E_y}\Delta\beta = \frac{1}{2}\sin(2\beta)(d_{21} - d_{23}) - \sin^2(\beta)\ d_{25}. \tag{10}$$

Since equations (7)–(10) relate the unit cell deformation with the piezoelectric coefficients, one has to associate these deformations to the multiple diffraction secondary peak position in a Renninger scan.

3. Secondary peak position in a Renninger scan

In the multiple diffraction phenomenon a set of planes, usually parallel to the sample surface referred to primary planes (h_p, k_p, ℓ_p), are adjusted to diffract the incident beam. By rotating the sample by ϕ around the primary reciprocal lattice vector, several other secondary planes (h_s, k_s, ℓ_s) within the single crystal with arbitrary orientation also diffract. The interactions among the primary and several secondary reflections are established by the coupling reflections (h_p–h_s, k_p–k_s, ℓ_p–ℓ_s). These interactions appear in the I_{primary} versus ϕ pattern which is usually called a Renninger scan [8]. Due to both the n-fold symmetry of the chosen primary vector and the two diffraction conditions represented by the entrance and exit of the secondary reciprocal lattice point on the Ewald sphere under rotation, the Renninger scan shows $2n$ mirrors of symmetry throughout the pattern. A review of this technique is presented elsewhere [9].

The angular position of a multiple diffraction peak corresponding to any [$h\,k\,\ell$] secondary plane for a fixed wavelength (λ), can be determined in terms of the angle $\phi \pm \phi_0$ (the signal $\pm$ defines the entrance and exit of the reciprocal secondary node from the Ewald sphere), where ϕ_0 is the angle between the secondary vector and the primary incidence plane measured in the Ewald sphere equatorial plane [10]. This angular position is given by

$$\cos\left(\phi^{h\,k\,\ell} \pm \phi_0\right) = \frac{1}{2}\ \frac{(H^2 - \vec{H}\cdot\vec{H}_0)}{\sqrt{\frac{1}{\lambda^2} - \frac{H_0^2}{4}}\sqrt{H^2 - H_p^2}} \tag{11}$$

where $\vec{H}_0$ is the primary vector, $\vec{H}$ the secondary vector defined as $\vec{H}_{h\,k\,\ell} = h\vec{a}^* + k\vec{b}^* + \ell\vec{c}^*$ and $\vec{H}_p$ the coupling vector expressed by

$$\vec{H}_p = (\vec{H}\cdot\vec{H}_0)\left(\frac{\vec{H}_0}{H_0^2}\right).$$

In case of a monoclinic crystal, the primary and secondary vectors are

$$\vec{H}_0 = \frac{h_0}{a\ \sin\beta}\hat{a} + \frac{k_0}{b}\hat{b} + \frac{\ell_0}{c\ \sin\beta}\hat{c} \qquad \vec{H}_{h\,k\,\ell} = \frac{h}{a\ \sin\beta}\hat{a} + \frac{k}{b}\hat{b} + \frac{\ell}{c\ \sin\beta}\hat{c}. \tag{12}$$

By considering $(h_0\,0\,0)$ as the primary reflection, the angular peak position given in equation (11) assumes the form

$$\cos\left(\phi^{h\,k\,\ell} \pm \phi_0\right) = \frac{1}{2}\frac{\frac{h(h-h_0)}{a^2\,\sin^2\beta} + \frac{k^2}{b^2} + \frac{\ell^2}{c^2\,\sin^2\beta} - \frac{\ell(2h-h_0)\,\cos\beta}{ac\,\sin^2\beta}}{\sqrt{\frac{1}{\lambda^2} - \frac{h_0^2}{4a^2\,\sin^2\beta}}\;\sqrt{\frac{\ell^2}{c^2} + \frac{k^2}{b^2}}} = f(a,\,b,\,c,\,\beta). \tag{13}$$

Thus, in order to relate the lattice deformation with the peak position this equation should be differentiated to give

$$-\sin\left(\phi^{h\,k\,\ell} \pm \phi_0\right)\Delta\left(\phi^{h\,k\,\ell} \pm \phi_0\right) = \left.\frac{\partial f}{\partial a}\right|_{h\,k\,\ell}\Delta a + \left.\frac{\partial f}{\partial b}\right|_{h\,k\,\ell}\Delta b + \left.\frac{\partial f}{\partial c}\right|_{h\,k\,\ell}\Delta c + \left.\frac{\partial f}{\partial \beta}\right|_{h\,k\,\ell}\Delta\beta. \tag{14}$$

Since the primary reflection is $(h_0\,0\,0)$, the variation in the lattice parameter a is given by Bragg's law of differentiation

$$\frac{\Delta a}{a} = -\cot(\omega_{h\,0\,0})\Delta\omega - \cot(\beta)\Delta\beta. \tag{15}$$

By adding (7) and (10) one has

$$\frac{\cos\beta}{E_y}\left(\frac{\Delta\beta}{\sin\beta} + \frac{\Delta a}{a\,\cos\beta}\right) = d_{21} \tag{16}$$

which can be simplified by using (15) to give

$$d_{21} = -\frac{\cot(\omega_{h\,0\,0})\Delta\omega}{E_y}. \tag{17}$$

The other coefficients are obtained by choosing the appropriate secondary reflection; for instance,

1. Secondary $(0\,k\,0)$

$$\frac{\Delta b}{b}\left(\left.\frac{\partial f}{\partial b}\right|_{0\,k\,0}\right) = \tan\left(\phi^{0\,k\,0} \pm \phi_0\right)\Delta\left(\phi^{0\,k\,0} \pm \phi_0\right) - \frac{\Delta a}{a}\left.\frac{\partial f}{\partial a}\right|_{0\,k\,0} - \Delta\beta\left.\frac{\partial f}{\partial \beta}\right|_{0\,k\,0}. \tag{18}$$

2. Secondary $(0\,0\,\ell)$

$$\frac{\Delta c}{b}\left(\left.\frac{\partial f}{\partial c}\right|_{0\,0\,\ell}\right) = \tan\left(\phi^{0\,0\,\ell} \pm \phi_0\right)\Delta\left(\phi^{0\,0\,\ell} \pm \phi_0\right) - \frac{\Delta a}{a}\left.\frac{\partial f}{\partial a}\right|_{0\,0\,\ell} - \Delta\beta\left.\frac{\partial f}{\partial \beta}\right|_{0\,0\,\ell}. \tag{19}$$

3. Secondary $(h\,0\,\ell)$

$$\Delta\beta\left(\left.\frac{\partial f}{\partial c}\right|_{h\,0\,\ell}\right) = \tan\left(\phi^{h\,0\,\ell} \pm \phi_0\right)\Delta\left(\phi^{h\,0\,\ell} \pm \phi_0\right) - \frac{\Delta a}{a}\left.\frac{\partial f}{\partial a}\right|_{h\,0\,\ell} - \frac{\Delta c}{c}\left.\frac{\partial f}{\partial c}\right|_{h\,0\,\ell}. \tag{20}$$

The piezoelectric coefficients for a monoclinic crystal are obtained after the substitution of the lattice parameter variation in the corresponding equations (7)–(10).

4. Experimental details

The data collection for this study was carried out using the Renninger scanning geometry developed in a P4 SIEMENS single crystal diffractometer by adding a long pipe evacuated collimator which provides a low divergence incident beam. The divergences obtained with this geometry are $\delta_{\rm v} = 107$ arc seconds in the vertical plane and $\delta_{\rm h} = 149$ arc seconds in the horizontal plane. The radiation used was Cu Kα(1) for the Renninger scans and Cu Kβ for the rocking curves and the measurements were performed with step sizes of 0.0008° and 0.005° in the ω and ϕ axes, respectively. The $(6\,0\,0)$ rocking curve was measured for most of

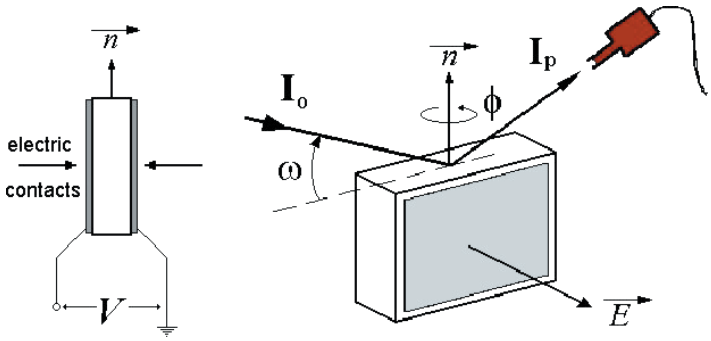

Figure 1. Scheme of the electric field applied in the sample to allow for piezoelectric coefficient determination using XRMD. The normal $\vec{n}$ to the primary reflection planes and the *E*-direction are indicated in the figure.

the cases and it was chosen as the primary reflection for the Renninger scan measurements. The (8 0 0) rocking curve was also measured in one case.

The typical sizes of the samples used in this paper were 5.0 mm × 2.5 mm × 1.5 mm (the smallest being the face where the x-ray incident beam diffracts) and the electric field was applied in the [0 1 0] direction; it means that $\vec{E}$ is parallel to the $\vec{b}$-axis. The electric field was generated by a variable voltage, low current dc power supply and was applied to the samples via wires running from the power supply to small bolts attached to the metal tabs of the sample holder. A conductive sponge (kindly supplied by SGL Carbon Group, Meitingen, Germany) was positioned between the tabs and the sample just to improve electrical contact, to generate a uniform field within the sample and, to prevent the mechanical strain in the sample due to contact with the metallic plates, as shown in figure 1.

In this figure, the incidence angle (ω), the rotation angle (ϕ), the normal $\vec{n}$ to the primary planes and the $\vec{E}$ direction are also depicted. I_0 represents the incidence beam and I_p the diffracted primary beam.

5. Results and discussion

The Renninger scan measurements were carried out for different Rochelle salt samples in the orthorhombic phase ($T > 24$ °C) and a typical region of the (6 0 0) scan around the $\phi = 0°$ symmetry mirror is shown in figure 2. Once the weak (6 0 0) reflection was chosen as the primary reflection for the Renninger scan measurements, it just shows positive peaks that make the alignment of the samples and the piezoelectric coefficient measurements easier. The indexing of the secondary reflections appearing in the scan is provided for the reference vector [0 1 0]. The occurrence of the Laue (transmitted) three-beam case (1 1 2), two BSD cases (3 0 2) and (3 1 2) appearing 0.107° apart from each other and the (2 0 1)(4 0 1) Laue–Bragg four-beam case on one side of the mirror together with their corresponding mirrored reflections can be observed.

In order to study the effect of the electric field parallel to $\vec{b}$-axis in the Rochelle salt the sample was kept at $T \approx 22$ °C in the ferroelectric phase. The (8 0 0) rocking curves were measured for the *E* values varying up to 1.1×10^5 V m^{-1} and the results are depicted in figure 3. The peak shape is kept the same indicating a uniform strain within the sample whereas its angular position clearly changes towards the high angles even under the application of low electric field values. The maximum peak positions were transformed into lattice strain through

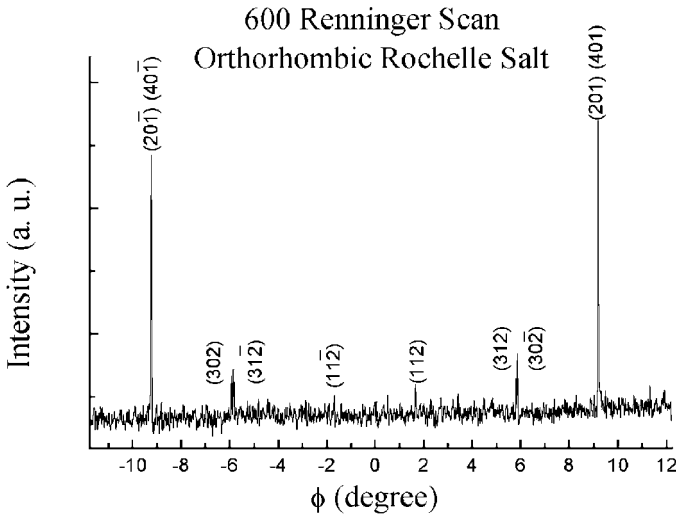

Figure 2. Portion of the 6 0 0 Rochelle salt Renninger scan around the $\phi = 0^\circ$ symmetry mirror in the orthorhombic phase.

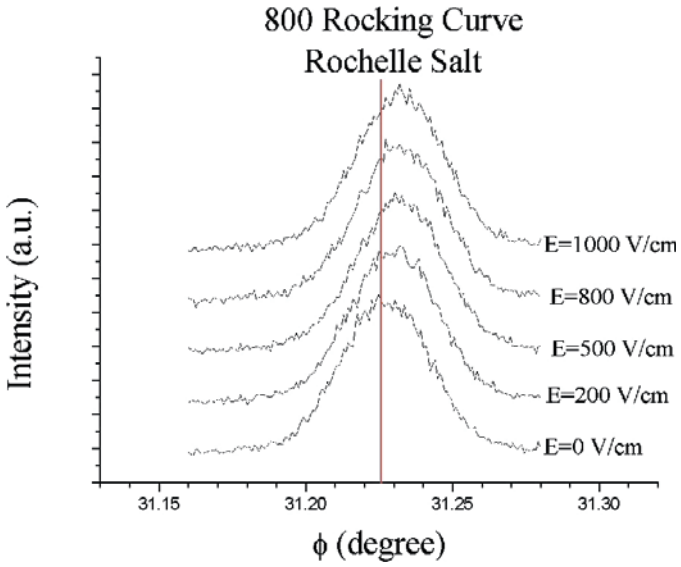

Figure 3. Peak shift in the 8 0 0 Rochelle salt rocking curves under electric field.

equation (17) and the result as a function of the electric field appears in figure 4. The d_{21} piezoelectric coefficient is obtained from this figure as $7.0(6) \times 10^{-10}$ CN^{-1}. It should be pointed out that analogous rocking curve measurements using the (6 0 0) weaker reflection were performed and have provided the result $d_{21} = 9(1) \times 10^{-10}$ CN^{-1} which agrees reasonably well with the previous result although with lower precision in the peak shift determination.

In order to illustrate the useful versatility of the multiple diffraction phenomenon in the determination of several piezoelectric coefficients of the Rochelle salt, the measurement of the three-beam case (0 0 0)(6 0 0)(2 0 2) in which the secondary Laue reflection (2 0 2) is

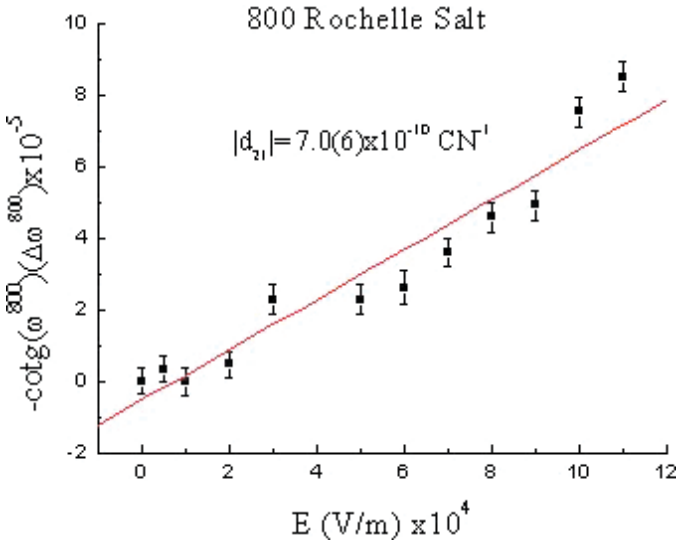

Figure 4. Rochelle salt lattice strain obtained from the 8 0 0 rocking curves as a function of the electric field, which yields the piezoelectric coefficient d_{21}.

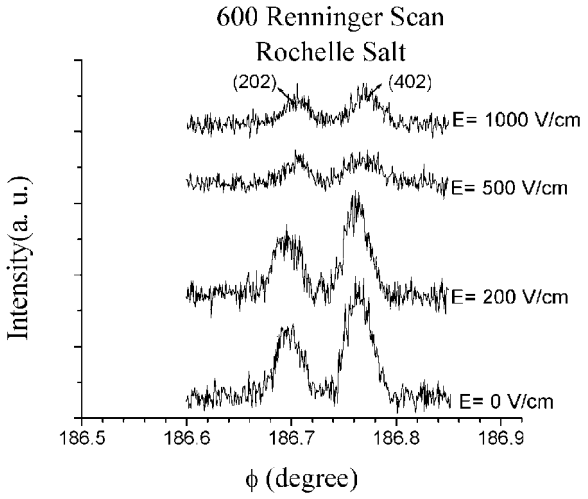

Figure 5. Electric field effect in the 6 0 0 Renninger scan secondary peaks (2 0 2) and (4 0 2).

associated with the d_{25} coefficient is shown in figure 5. Since this peak appears to be close ($\Delta\phi = 0.21^{\circ}$) to the three-beam Bragg–Bragg case (0 0 0)(6 0 0)(4 0 2) we decided to show both in the same measured portion of the Renninger scan under the E application. This measurement indicates that we are able to measure the effect of the electric field in two (even more) distinct reflections at the same time.

The measurement of the three-beam case involving the Laue secondary reflection (0 0 1) at $\phi = 187.41^{\circ}$ under the E application in conjunction with equation (9) gives $d_{23} = 2.1(9)\times 10^{-9}$ CN^{-1}. By working with equations (7) and (10) and using the d_{23} value we can plot the resultant lattice strain as a function of E to obtain $d_{25} = 3.7(8) \times 10^{-11}$ CN^{-1} as shown in figure 6. It should be pointed out that the value obtained for the d_{25} agrees well with the

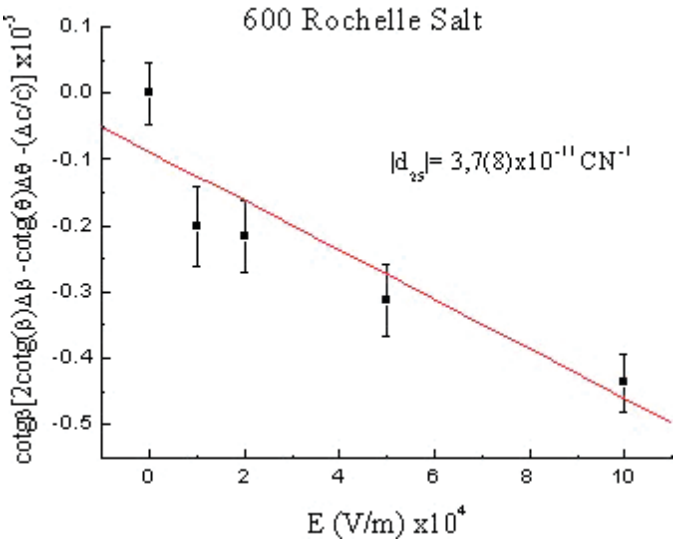

Figure 6. Rochelle salt lattice strain obtained from (0 0 0)(6 0 0)(2 0 2) three-beam peak shift as a function of the electric field to give rise to the piezoelectric coefficient d_{25}.

literature [11] value of 5.3×10^{-11} CN^{-1}. The last piezoelectric coefficient d_{22} in the tensor row, for E parallel to [0 1 0], has been obtained as $2.2(9)\times 10^{-9}$ CN^{-1}, from the measurement of the (0 1 0) secondary peak shift in the (6 0 0) Renninger scan and equation (9).

6. Conclusions

0The successful application of the XRMD method with enough sensitivity to act as a three-dimensional probe to detect small Rochelle salt lattice deformations induced by the electric field parallel to the *b*-axis is shown in this paper. Furthermore, it was used in the determination of several piezoelectric coefficients for Rochelle salt obtained from just one Renninger scan.

The necessary modifications in the multiple diffraction theory in order to account for the Rochelle salt case in which one has a different primary reflection, and also the relationship with the converse piezoelectric effect have been presented.

The results obtained for the Rochelle salt piezoelectric coefficients using the multiple diffraction method show that, by no means, the sample direction in which E is applied makes a great difference in the values of the piezoelectric coefficients.

Acknowledgments

The authors thank the Brazilian Agencies FAPESP, FUNCAP, CNPq and FAEP/UNICAMP for financial support.

References

[1] Solnas X, Gonzales-Silgo C and Ruiz-Pérez C 1997 *J. Solid State Chem.* **131** 350
[2] Cady W G 1946 *Piezoeletricity* (New York: Dover) edited review 1964
[3] Special issue on piezoelectricity 1982 *Ferroelectrics* **40–43**
[4] Vigness C I 1934 *Phys. Rev.* **46** 255

[5] Avanci L H, Cardoso L P, Girdwood S E, Pugh D, Sherwood J N and Roberts K J 1998 *Phys. Rev. Lett.* **81** 5426
[6] Avanci L H, Cardoso L P, Sasaki J M, Girdwood S E, Roberts K J, Pugh D and Sherwood J N 2000 *Phys. Rev.* B **61** 6507
[7] Nye J F 1957 *Physical Properties of Crystals* Oxford Science Publications (Oxford: Clarendon)
[8] Renninger M 1937 *Z. Phys.* **106** 141
[9] Chang S L 1984 *Multiple Diffraction of X-Rays in Crystals (Springer Series Solid-State Science vol 50)* (Berlin: Springer)
[10] Cole H, Chamber F W and Dunn H M 1962 *Acta Crystallogr.* **15** 138
[11] Shuvalov L A 1988 *Modern Crystallography IV* (Berlin: Springer) p 234